RESEARCH ARTICLE | MAGNETISM AND MAGNETIC MATERIALS | JANUARY 27 2014

Giant electric-field-induced magnetic anisotropy reorientation with patterned electrodes on a Ni thin film/lead zirconate titanate heterostructure

Jizhai Cui; Joshua L. Hockel; Paul K. Nordeen; David M. Pisani; Gregory P. Carman; Christopher S. Lynch

J. Appl. Phys. 115, 17C711 (2014)
https://doi.org/10.1063/1.4863258

Giant electric-field-induced magnetic anisotropy reorientation with patterned electrodes on a Ni thin film/lead zirconate titanate heterostructure

Jizhai Cui, Joshua L. Hockel, Paul K. Nordeen, David M. Pisani, Gregory P. Carman, and Christopher S. Lynch[a)]
Department of Mechanical and Aerospace Engineering, University of California, Los Angeles, California 90095, USA

(Presented 8 November 2013; received 23 September 2013; accepted 28 October 2013; published online 27 January 2014)

This study reports a method of using patterned electrodes on a piezoelectric substrate to generate local strain to control magnetic properties of individual magnetic units. By operating different effective electrode pairs on a piezoelectric substrate, a local bi-axial strain is generated. This rotates the magnetic anisotropy of a 35 nm thick and 0.5 mm diameter Ni island through the magnetoelastic effect. The electric-field-induced magnetic anisotropy exhibits an anisotropy field up to 600 Oe and a 75% change in magnetic remanence. © *2014 AIP Publishing LLC*.
[http://dx.doi.org/10.1063/1.4863258]

Manipulating magnetization using electric field in multiferroic materials has many possible device applications, such as magnetic random access memory (MRAM).[1] Magnetoelectric (ME) heterostructures have high coupling between electric polarization and magnetization, the multiferroic order parameters.[2] In the strain-mediated magnetoelectric effect, an electric field applied to the piezoelectric layer generates strain that couples directly to a magnetic layer. Several studies have reported magnetization reorientation[3–7] and magnetic coercive field changes[8] in strain-mediated ME heterostructures. The majority of prior work only demonstrated that strain can rotate the magnetization vector but offered no possibility of controlling individual magnetic islands on the surface of a thin film because the piezoelectric strain was uniform throughout the piezoelectric layer. Further, the previously used approach may not be applicable to a thin film piezoelectric grown on a Si or other substrate because the much thicker substrate clamps the in-plane component of the strain. The result of using a monolithic piezoelectric substrate with the entire surface electrode is that all magnetic surface elements are subjected to the same strain field and rotate simultaneously. A method is needed to control individual magnetic islands on the surface of a thin film piezoelectric.

We report such a method based on using patterned electrodes to induce localized strain in a piezoelectric substrate. This approach is demonstrated to control the magnetic anisotropy of a single magnetic unit. The out-of-plane (d_{33}) expansion and in-plane (d_{31}) contraction of the region immediately under the electrodes produce a highly localized strain field that affects the region surrounding the electrodes. The patterned electrodes around a magnetostrictive island are shown in Figure 1. With the bottom electrode grounded, when applying positive voltage to a pair of top electrodes (either A-A or B-B), a local electric field E along the z axis is generated as shown Fig. 1(a). The piezoelectric material underneath the electrodes elongates out-of-plane (z axis) and contract in-plane (x and y axis) due to the d_{31} piezoelectric effect. Strain-displacement compatibility requires that the piezoelectric strain be compatible with the overall strain field resulting in a mechanical stretching of the material between the surface electrodes to accommodate the piezoelectric in-plane contraction under the electrodes. When voltage is applied to electrodes A-A as shown in Fig. 1(b), the magnetic element is elongated along the x direction ($\varepsilon_{xx} > 0$) and is contract along the y direction ($\varepsilon_{yy} < 0$), a local bi-axial strain ($\varepsilon_{xx} - \varepsilon_{yy} > 0$). Likewise, if electrodes B-B are activated, the magnetic element will experience elongation along the y direction ($\varepsilon_{yy} > 0$) and contraction along x direction ($\varepsilon_{xx} < 0$). The result is that the strain field is rotated by 90°, i.e., $\varepsilon_{xx} - \varepsilon_{yy} < 0$. The net bi-axial strain $\Delta\varepsilon = \varepsilon_{xx} - \varepsilon_{yy}$ induces the in-plane magnetoelastic anisotropy necessary for control of individual magnetic islands in strain-coupled ME heterostructures.[9,10] We used linear piezoelectric finite element analysis (FEA) to analyze the effect of electrode pattern on local strain. Properties of lead zirconate titanate (PZT-5H) with $d_{33} = 690\ \text{pCN}^{-1}$ and $d_{31} = -340\ \text{pCN}^{-1}$ were given to piezoelectric substrate. The electrode geometry was $0.6 \times 0.6\ \text{mm}^2$ for electrode spacing $L = 1.0\,\text{mm}$. 1.5 kV (3 MV m^{-1} through the substrate thickness $t = 0.5\,\text{mm}$) was applied to an electrode pair with the bottom surface grounded. As shown in Fig. 1(d), positive ε_{xx} and negative ε_{yy} strain fields are generated between electrodes, which is appropriate for generating magnetoelastic anisotropy on magnetic elements. Additionally, it shows that only a small region surrounding the electrodes is strained, thus enabling application to arrays of indexed magnetic elements.

In experiments, the substrate consisted of a polished $10 \times 10 \times 0.5\ \text{mm}^3$ PZT-5H with piezoelectric constants $d_{33} = 690\ \text{pCN}^{-1}$ and $d_{31} = -340\ \text{pCN}^{-1}$. As shown in Fig. 1(c), the fabricated electrode pads were squares with lateral size $d = 0.6\,\text{mm}$ and inter-pad spacing $L = 1.0\,\text{mm}$, which are same as the parameters used in FEA simulations. A small strip as an add-on of the pads was used for electric connection. The diameter of the Ni disc was 0.5 mm. Films of 3 nm

a)Electronic mail: cslynch@seas.ucla.edu

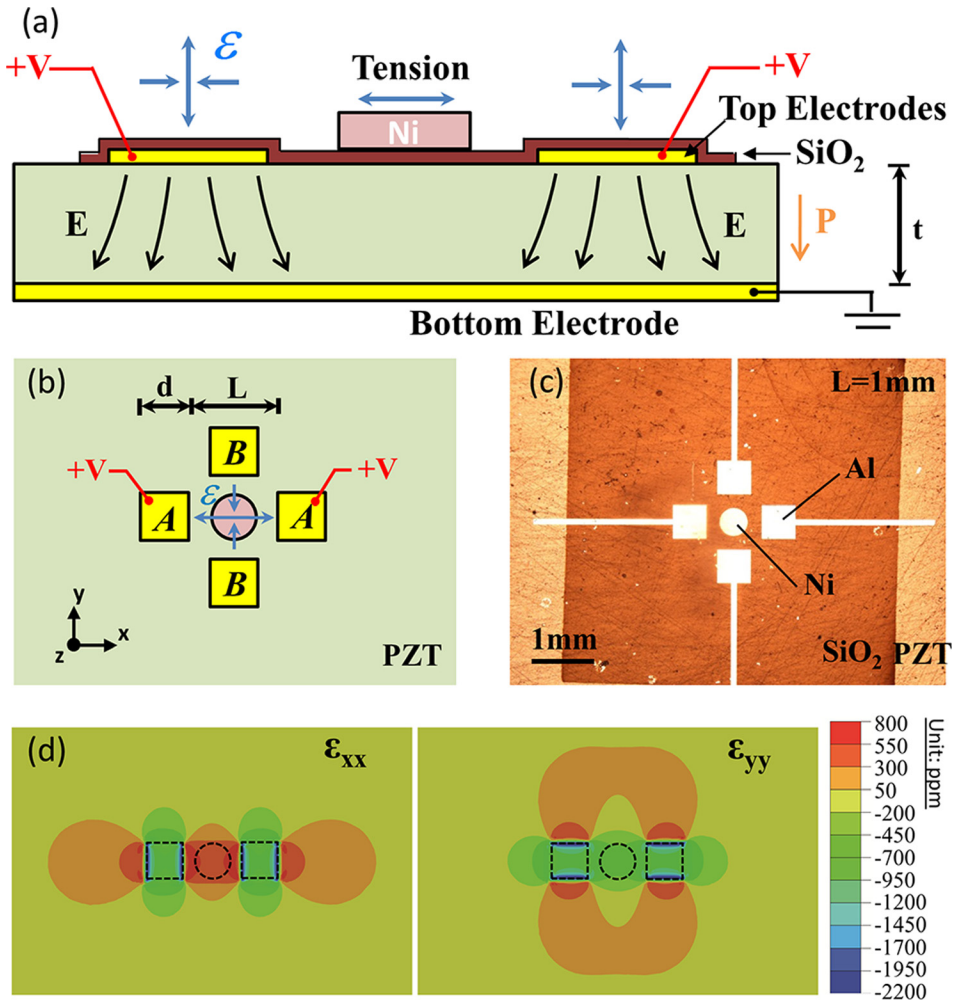

FIG. 1. Schematic of device structure and operation method for generating local bi-axial surface strain. (a) Cross section and (b) top view. (c) Top view of fabricated patterned electrodes and Ni element on PZT observed by an optical microscope. (d) Top views of FEA simulation of 1.5 kV applied to an electrode pair with substrate bottom surface grounded. The dashed line squares and circle indicate the location of electrodes and magnetic elements, respectively.

Ti as adhesion layer and 100 nm Al electrodes were deposited by e-beam evaporation. 50 nm SiO_2 was next evaporated to create an insulating layer to reduce the likelihood of electric breakdown between the pads. Finally, by the same technique, a film of 3 nm Ti/35 nm Ni was deposited. The circular disc geometry of Ni reduced asymmetry that might directionally interfere with magnetization changes. The SiO_2 layer was used to screen charge, reducing the influence of a charge-induced ME effect on the measured magnetization changes.[11,12] Longitudinal magneto-optical Kerr effect (MOKE) magnetometry was used to measure the electric field induced magnetic anisotropy of the Ni disc. The direction of the laser beam (measurement of Kerr rotation) was always parallel to the direction of applied magnetic field. The laser beam diameter was tuned to 0.5 mm, identical to the diameter of the Ni disc. Hence the MOKE measurement represents an averaged magnetic response.

Figure 2 shows the normalized Kerr rotation hysteresis curves (M-H) of the initial state (i.e., no voltage applied) and states with applied voltages on A-A electrodes. Comparing the initial state in Figs. 2(a) and 2(b), the saturation magnetic field levels were similar along the x and y axes, indicating a lack of preferred easy and hard axes before voltage was applied. The M-H curves for the initial state also showed a large remanent magnetization $M_r/M_S = 95\%$ in both the x and y directions. When applying voltages of 0.5 kV, 1.0 kV, and 1.5 kV on A-A electrodes successively along the x axis, the anisotropy field of the hysteresis curves was increased while the remanent magnetization was decreased, as shown in Fig. 2(a). With 1.5 kV applied, the Ni island displayed a large anisotropy field up to $H_a = 600$ Oe and magnetic remanence as low as $M_r/M_S = 25\%$, a 70% decrease from the initial state. These indicate an induced hard axis along the x axis. The M-H curves along the y axis in Fig. 2(b) display an increased coercivity H_c with 100% zero field remanence, indicating an induced easy axis along the y axis. As described in Fig. 1, applying voltages on A-A induces a bi-axial strain field of $\varepsilon_{xx} - \varepsilon_{yy} > 0$ between electrodes. Due to the negative magnetostriction of Nickel, the bi-axial strain field induces a hard axis along the x axis and an easy axis along y axis.[13] The dependence of anisotropy field H_a and coercivity H_c on applied voltages was observed. Higher voltages (electric field) generated larger strain response on the Ni element, thus inducing increased H_a along x axis (hard axis) and H_c along y axis (easy axis). The experimental results are consistent with previous published studies.[4,5]

Figure 3 shows the M-H curves when voltages are applied on B-B after applying voltages on A-A. In Fig. 3(b), the measured M-H curves between the activated electrodes, i.e., the y axis when applying voltages on B-B, showed an increased anisotropy field ($H_a = 600$ Oe under 1.5 kV) and lowered remanent magnetization $M_r/M_S = 20\%$ under 1.5 kV, a 75% decrease from the initial state. Higher coercive field H_c curves with 100% remanence were observed

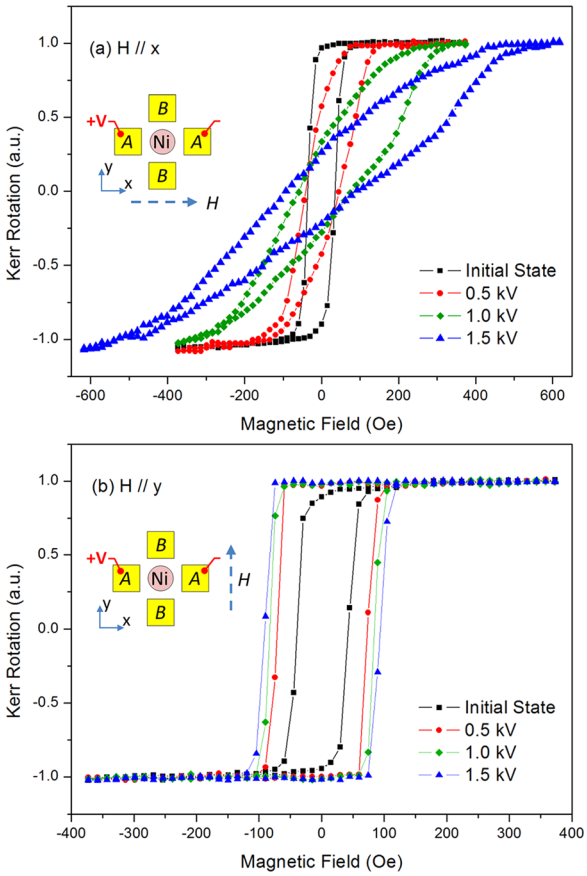

FIG. 2. Normalized Kerr rotation hysteresis curves (M-H) measured under different applied voltages on A-A electrodes. (a) M-H along x direction with magnetic field along x direction and (b) M-H along y direction with magnetic field along y direction.

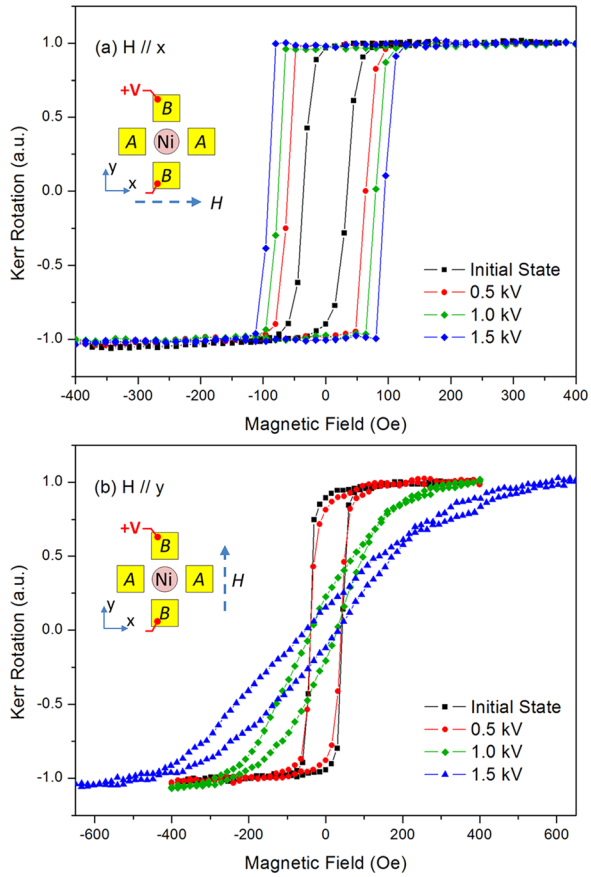

FIG. 3. Normalized Kerr rotation hysteresis curves (M-H) measured under different applied voltages on B-B electrodes. (a) M-H along x direction with magnetic field along x direction and (b) M-H along y direction with magnetic field along y direction.

along the x axis as shown in Fig. 3(a). The results indicate that the y axis became the hard axis and the x axis the easy axis, which is opposite to the A-A electrode case. That is to say, the direction of electric-field-induced magnetic anisotropy was rotated 90° by application of voltage to B-B instead of A-A. This is because the induced bi-axial strain is $\varepsilon_{xx} - \varepsilon_{yy} < 0$, which is also rotated by 90 degrees comparing $\varepsilon_{xx} - \varepsilon_{yy} > 0$ when the A-A electrodes were activated. A similar trend was observed for the voltage dependence of the anisotropy field and coercive field.

In conclusion, we have demonstrate that using patterned electrodes on a piezoelectric substrate can be used to generate local strain and induce and reorient magnetic anisotropy in a 35 nm thick and 0.5 mm diameter Ni island. By operating effective electrode pairs, different local bi-axial strain fields can be generated to tune the magnetic properties of the Ni film. This approach may be suitable for next generation MRAM devices with low writing energy and fast writing speed. Our results suggest that this approach has the potential to be scaled down to the micro- or nano-scale and used to achieve local in-plane strain on the surface of piezoelectric thin films subject to substrate clamping.

The authors would like to thank Wen Dong, Sam Goljahi, and Dr. William T. J. McFinnister for their valuable discussions. This work was supported by NSF Nanosystems Engineering Research Center for Translational Applications of Nanoscale Multiferroic Systems (TANMS) Cooperative Agreement Award EEC-1160504.

[1]W. Eerenstein, N. D. Mathur, and J. F. Scott, Nature **442**(7104), 759 (2006).
[2]C. W. Nan, M. I. Bichurin, S. X. Dong, D. Viehland, and G. Srinivasan, J. Appl. Phys. **103**(3), 031101 (2008).
[3]M. Liu, O. Obi, J. Lou, Y. J. Chen, Z. H. Cai, S. Stoute, M. Espanol, M. Lew, X. Situ, K. S. Ziemer, V. G. Harris, and N. X. Sun, Adv. Funct. Mater. **19**(11), 1826 (2009).
[4]T. Wu, A. Bur, P. Zhao, K. P. Mohanchandra, K. Wong, K. L. Wang, C. S. Lynch, and G. P. Carman, Appl. Phys. Lett. **98**(1), 012504 (2011).
[5]T. Wu, A. Bur, W. Kin, Z. Ping, C. S. Lynch, P. K. Amiri, K. L. Wang, and G. P. Carman, Appl. Phys. Lett. **98**(26), 262504 (2011).
[6]J. L. Hockel, A. Bur, T. Wu, K. P. Wetzlar, and G. P. Carman, Appl. Phys. Lett. **100**(2), 022401 (2012).
[7]Y. Dusch, N. Tiercelin, A. Klimov, S. Giordano, V. Preobrazhensky, and P. Pernod, J. Appl. Phys. **113**(17), 17C719 (2013).
[8]J. Wang, J. Ma, Z. Li, Y. Shen, Y. Lin, and C. W. Nan, J. Appl. Phys. **110**(4), 043919 (2011).
[9]M. Weiler, A. Brandlmaier, S. Geprägs, M. Althammer, M. Opel, C. Bihler, H. Huebl, M. S. Brandt, R. Gross, and S. T. B. Goennenwein, New J. Phys. **11**(1), 013021 (2009).
[10]M. Buzzi, R. V. Chopdekar, J. L. Hockel, A. Bur, T. Wu, N. Pilet, P. Warnicke, G. P. Carman, L. J. Heyderman, and F. Nolting, Phys. Rev. Lett. **111**(2), 027204 (2013).
[11]Z. Li, J. Hu, L. Shu, Y. Gao, Y. Shen, Y. Lin, and C. W. Nan, J. Appl. Phys. **111**(3), 033918 (2012).
[12]J.-M. Hu, C.-W. Nan, and L.-Q. Chen, Phys. Rev. B **83**(13), 134408 (2011).
[13]R. C. O'Handley, *Modern Magnetic Materials: Principles and Applications* (Wiley, New York, 2000).